Broad tuning of whispering-gallery modes in silicon microdisks

Jeffrey M. Shainline[1], **Gustavo Fernandes**[2], **Zhijun Liu**[2], **and Jimmy Xu**[1,2]

[1]*Department of Physics and* [2]*Division of Engineering, Brown University, 184 Hope St., Providence, RI, 02912*

Jeffrey.Shainline@gmail.com

Abstract: Silicon microdisks with dynamically-tunable resonance spectra are achieved with nanoscale, in-plane silicon electrical contacts in a single lithographic step. Electrical current is passed through the devices to enable thermal tuning via joule heating. A 14nm wavelength shift is demonstrated with 1.6mW power consumption in devices with >20nm free spectral ranges and quality factors exceeding 20,000. Spectral shifts equal to a full width at half maximum can be achieved with $\sim 10\mu$W tuning power for a mode with quality factor of 20,000.

OCIS codes: (230.5750) Resonators, (250.5300) Photonic integrated circuits, (130.3990) Micro-optical devices, (130.3120) Integrated optics devices

References and links

1. Q. Xu, S. Manipatruni, B. Schmidt, J. Shakya, and M. Lipson, "12.5 Gbit/s carrier-injection-based silicon microring silicon modulators," Opt. Express **15**, 430–436 (2007).
2. S. Manipatruni, Q. Xu, B. Schmidt, J. Shakya, and M. Lipson, "High speed carrier injection 18 Gb/s silicon micro-ring electro-optic modulator," in "The 20th Annual Meeting of the IEEE Lasers and Electro-Optics Society," (2007), pp. 537–538.
3. S. Manipatruni, R. Dokania, B. Schmidt, N. Sherwood-Droz, C. Poitras, A. Apsel, and M. Lipson, "Wide temperature range operation of micrometer-scale silicon electro-optic modulators," Opt. Lett. **33**, 2185–2187 (2008).
4. M. R. Watts, D. C. Trotter, R. W. Young, and A. L. Lentine, "Ultralow power silicon microdisk modulators and switches," in "Proc. IEEE 2008 Int. Meeting Group IV Photon.", (Sorrento, Italy, 2008), pp. 4–6.
5. I. Fushman, E. Waks, D. Englund, N. Stoltz, P. Petroff, and J. Vuckovic, "Ultrafast nonlinear optical tuning of photonic crystal cavities," Appl. Phys. Lett. **90**, 091118 (2007).
6. M. Benyoucef, S. Kiravittaya, Y. F. Mei, A. Rastelli, , and O. G. Schmidt, "Strongly coupled semiconductor microcavities: a route to couple artificial atoms over micrometric distances," Phys. Rev. B **77**, 035108 (2008).
7. K. Srinivasan and O. Painter, "Optical fiber taper coupling and high-resolution wavelength tuning of microdisk resonators at cryogenic temperatures," Appl. Phys. Lett. **90**, 031114 (2007).
8. M. Humar, M. Ravnik, S. Pajk, and I. Muevi, "Electrically tunable liquid crystal optical microresonators," Nature Photonics **3**, 595–600 (2009).
9. I. Frank, P. Deotare, M. McCutcheon, and M. Loncar, "Programmable photonic crystal nanobeam cavities," Opt. Express **18**, 8705–8712 (2010).
10. P. T. Rakich, M. A. Popovic, M. R. Watts, T. Barwicz, H. I. Smith, and E. P. Ippen, "Ultrawide tuning of photonic microcavities via evanescent field perturbation," Opt. Lett. **31**, 1241–1243 (2006).
11. D. Arani, B. Min, A. Martin, and K. J. Vahala, "Electrical thermo-optic tuning of ultrahigh-Q microtoroid resonators," Appl. Phys. Lett. **85**, 5439–5441 (2004).
12. N. Sherwood-Droz, H. Wang, L. Chen, B. G. Lee, A. Biberman, K. Bergman, and M. Lipson, "Optical 4x4 hitless silicon router for optical networks-on-chip (NoC)," Opt. Express **16**, 15915–15922 (2008).
13. Y. Varshni, "Temperature dependence of the energy gap in semiconductors," Physica **34**, 149–154 (1967).
14. J. Shainline, S. Elston, Z. Liu, G. Fernandes, R. Zia, and J. Xu, "Subwavelength silicon microcavities," Opt. Express **17**, 23323–23331 (2009).
15. M. Oxborrow, "Traceable 2-d finite element simulation of the whispering gallery modes of axisymmetric electromagnetic resonators," IEEE Trans. Microwave Theory Tech. **55**, 1209–1218 (2007).

#127156 - $15.00 USD Received 20 Apr 2010; revised 28 May 2010; accepted 7 Jun 2010; published 21 Jun 2010

16. M. Borselli, T.J. Johnson, and O. Painter, "Beyond the Rayleigh scattering limit in high-Q silicon microdisks: theory and experiment," Opt. Express **13**, 1515–1530 (2005).
17. M. Borselli, K. Srinivasan, P. Barclay, and O. Painter, "Rayleigh scattering, mode coupling, and optical loss in silicon microdisks," Appl. Phys. Lett. **85**, 3693–3695 (2004).

1. Introduction

Microdisk and microring resonators can operate as functional components in myriad optical devices. Applications include particle sensors, cavity QED, and photonic circuit elements including switches, modulators, filters, and lasers. The ability to tune the mode spectra of these central optical components enables a multitude of dynamic devices. The characteristics of circular cavity resonators that make them attractive for photonic applications are their small size, large free spectral range (FSR), high cavity quality factor (Q), and ease of fabrication. For large-scale integration, CMOS-compatible, planar silicon structures are advantageous. Any effort to enable tuning in optical microcavities for photonic device applications should retain these attributes.

A number of technologies have been demonstrated to tune optical microcavities. Each of these technologies has strengths and limitations and may find applicability in certain contexts. Carrier injection via a p-i-n junction in a silicon microring [1-3], microdisk [4] and photonic crystal cavity [5] has been achieved with fairly high Q ($\sim$20,000 [1]), is compatible with the silicon material platform [1-4], allows for fast modulation (18 Gb/s [2]), and can be energy efficient [4]. Laser heating [5, 6] allows for high Q and fairly broad tuning. N_2 adsorption has been utilized for high Q and high resolution tuning [7]. Tuning liquid crystal droplet resonators in a polymer matrix via an external electric field allows for broad tuning (20nm) and fairly high Q ($\sim 12,000$) [8]. Electromechanically-tuned photonic crystal nanobeams have recently been demonstrated with measured Q factors of 13,000, tuning range of 10nm, and low power consumption [9]. Mechanical insertion of a dielectric into the near field of a microring has been shown to achieve broad tuning [10]. Ultrahigh-Q toroid cavities have been tuned thermooptically with joule heating, but with tuning range of less than 1nm [11]. Many integrated photonic devices have utilized thermal tuning in resonators or waveguides separated from resistive heaters by cladding layers (see ref. [12] and references therein), but such a design requires heating of the resistive element, the cladding layer, and the optical layer. There remains a demand for an energy-efficient planar silicon device with simple fabrication and no moving parts which can be easily coupled to a waveguide, has broad tuning range, high Q, stable operation, and large packing density allowing for many adjacent devices to be tuned independently on a single chip.

In this work we present a new tunable microdisk design which achieves the aforementioned objectives. The device consists of a silicon microdisk with nanoscale ($\sim$200nm) contacts on either side, as shown in Fig. 1(a). The large thermooptic coefficient of silicon ($1.86\times10^{-4}\mathrm{K}^{-1}$), due to the temperature dependence of the silicon bandgap [13], is leveraged to enable modal tuning via joule heating. The principle behind the design is to improve energy efficiency by passing current directly through the optically-active region rather than utilizing an external resistive heater. The device has broad tuning range (>14nm demonstrated) with mW tuning power, a simple, CMOS-compatible fabrication, and a well-defined mode spectrum with Q factors exceeding 20,000. The objective of the design is to achieve a versatile structure with low-power broad tuning and simple fabrication. More elaborate fabrication techniques [4, 10] may allow thermal, electrical, or mechanical tuning without placing contacts in the optical mode volume, but such a multi-mask fabrication is time consuming, expensive and, as we show here, not necessary for many applications. If an application only requires a mode shift by a single full width at half maximum, operation of this device can be achieved at powers of approximately

#127156 - $15.00 USD Received 20 Apr 2010; revised 28 May 2010; accepted 7 Jun 2010; published 21 Jun 2010

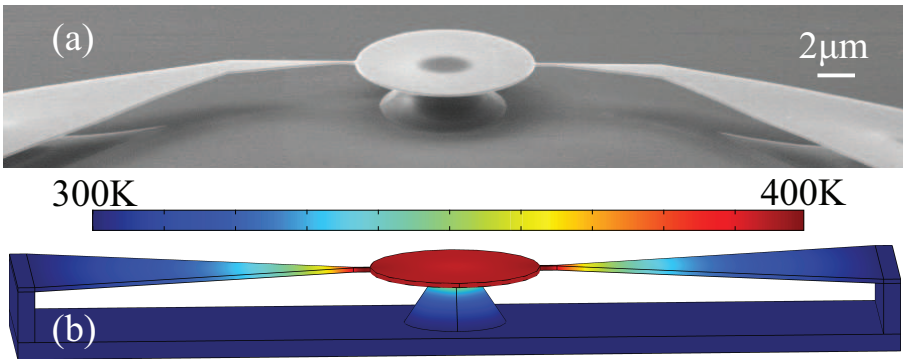

Fig. 1. (Color online) Microdisk structure with electrical contacts. (a) SEM image of the structure under consideration. (b) Electro-thermal simulation data. The surface temperature of the structure is shown.

10μW with less than 3V. For broader tuning on the order of a FSR, one only needs $\sim$1mW of power. In contrast to other tuning designs where a microheater is separated from the resonant element by a cladding layer, our design can leave the resonator exposed to the environment enabling it to be used as a sensor. Limitations of the design are that the point contacts scatter light from the optical mode reducing the photon lifetime, and applications that require fast switching will be constrained by the time required to heat and cool the disk. While thermal tuning is not generally competitive in ultrafast applications such as high-speed modulation [1-4], many devices such as sensors for particles with discrete absorption lines and tunable on-chip lasers may benefit from this structure. The device also enables coupling of narrow-line emitters with cavity modes in cavities with small mode volumes, high Qs, and large FSRs. Further, the fabrication of this device is an important result in that it introduces an entirely new technique to tune individual microcavities, it marks a new standard in energy efficiency of thermally-tuned microcavities, and it opens many possibilities for coupling electronic and optical degrees of freedom. Additionally, many photonic devices with coupled resonant elements suffer from sensitivity to fabrication imperfections. The tunable microdisks presented here offer a purely electrical, low-power means to tune coupled cavities into resonance with one another [6].

2. Modeling and fabrication

Calculations of whispering-gallery mode resonant wavelengths [14, 15] as a function of index of refraction inform us that $\sim$1nm of wavelength tuning can be achieved with a shift of 0.002 in the index of refraction. Shifting the resonances by 10nm requires changing the index of refraction from 3.48 to approximately 3.50. Silicon's relatively large thermooptic effect allows 10nm shifts to occur with a change of temperature of just over 100K. To anticipate the power required to achieve the desired tuning, the electro-thermal behavior of the device was modeled using Comsol Multiphysics. Figure 1(b) shows data from a simulation of a silicon microdisk based on a silicon-on-insulator (SOI) structure. The modeled disk has 10μm diameter contacted on either side by 200nm wide, 1μm long contacts. The contacts taper out to aluminum pads, one of which is held at a positive bias of 25V in the simulation and the other at ground. The aluminum pads and the silicon disk are isolated from the silicon wafer below by 3μm thick SiO_2 structures. All surfaces are allowed to radiate into air except the tops of the aluminum pads and the bottom of the underlying silicon wafer which are modeled as heat sinks held at 300K. This model suggests that 1.8mW of power dissipated in the device will raise the temperature by

#127156 - $15.00 USD Received 20 Apr 2010; revised 28 May 2010; accepted 7 Jun 2010; published 21 Jun 2010

100K. The simulations reveal that with this design the temperature of the disk can be raised very uniformly over the volume of the disk.

Devices are fabricated from SOI substrates (250nm device layer, 3μm buried oxide, Soitec). The first fabrication step is to implant the device layer with Boron to achieve the desired resistivity. The Comsol simulations inform us that the power dissipated in the device needed for broad tuning is $\sim$2mW. To achieve this power at 25V, the resistance of the device must be less than 625kΩ. Because we are aiming for Q factors of 10,000-20,000, and because the dominant contribution to photon decay will be scattering by the contacts, we can afford some photon lifetime degradation by free-carrier absorption and plasma losses due to doping. We achieve the desired trade-off between low resistivity and high Q by doping to a concentration of 10^{18} B^+/cm^3 which gives a resistivity of 0.04Ω·cm. At this carrier concentration we estimate the quality factor limited by free-carrier absorption and plasma losses to be on the order of 10^5. In practice, microdisks without contacts fabricated from substrates with such doping concentrations have modes with Q factors from 15,000-50,000, and final wired microdisk devices have resistance of approximately 250kΩ, thus satisfying our criteria that the resistance be less than 625kΩ and Q greater than 20,000 but indicating that less doping could lead to cavities with higher Q factors and still low enough resistances. Boron was implanted to a fluency of $2.5 \times 10^{13} B^+/cm^2$. Substrates were annealed in a N_2-purged furnace at 1000°C for 20min. Native oxide was removed and samples were coated with XR-1541 electron beam resist (Dow Corning) and disks of 10μm diameter with 200nm wide silicon electrodes leading to silicon pads for wire bonding were patterned. Etching was performed with ICP RIE using SF_6 and C_4F_8. The samples were cleaned with piranha etch and undercut with buffered hydrofluoric acid. The silicon samples were mounted on quartz chips patterned with gold regions for electrical contact. Wire bonds were made from the gold regions directly onto the silicon contact pads.

Several aspects of the device geometry can be modified depending on functionality needs and fabrication capacity. Our choice to undercut the disks to isolate the structures on pedestals was made for two reasons. First, it reduces the thermal contact to the substrate and therefore improves the energy efficiency. Second, the raised disk enables easier access for tapered fiber characterization. If one wishes to use on-chip waveguides, an undercut may still be performed, but care has to be taken to only undercut a small region around the disk so as to not lift off the entire waveguide. For non-undercut devices the drawback will be increased energy consumption, but the cooling time will be reduced. Our choice to have 200nm contacts was a compromise between high-Q, structural integrity, and low operating voltage. If one wishes to further improve the Q this can be achieved with a combination of increasing the resistivity of the substrate (by reducing ion implantation dosage) and reducing the width of the contacts. Both modifications will increase the overall resistance of the device and therefore lead to a higher operating voltage. If one can afford these costs, the Q factors can be improved substantially above those presented here. Additionally, the choice to fabricate tunable microdisks with wires directly in the microdisk sidewalls was motivated by the ease of fabrication. If one wishes only to utilize first-radial-order modes, a superior design would be either to pattern a metal ring at the center of the disk to be used as a heater or to pattern silicon wires which make contact to the inner wall of a microring resonator so that current is passed only through the ring where the optical mode resides. This is likely to be a highly energy efficient design and can be optimized to minimize interaction of the wire contacts with the optical mode. With a suitable design, either of these approaches could lead to broad tuning without contacting the region of the optical mode. The drawback is that in either of these cases contacts have to be made near the center of the structure, and these must be accessed by metal vias that rise up and over the region of the optical mode. This is likely to be at least a three-mask process which is best performed with

#127156 - $15.00 USD Received 20 Apr 2010; revised 28 May 2010; accepted 7 Jun 2010; published 21 Jun 2010

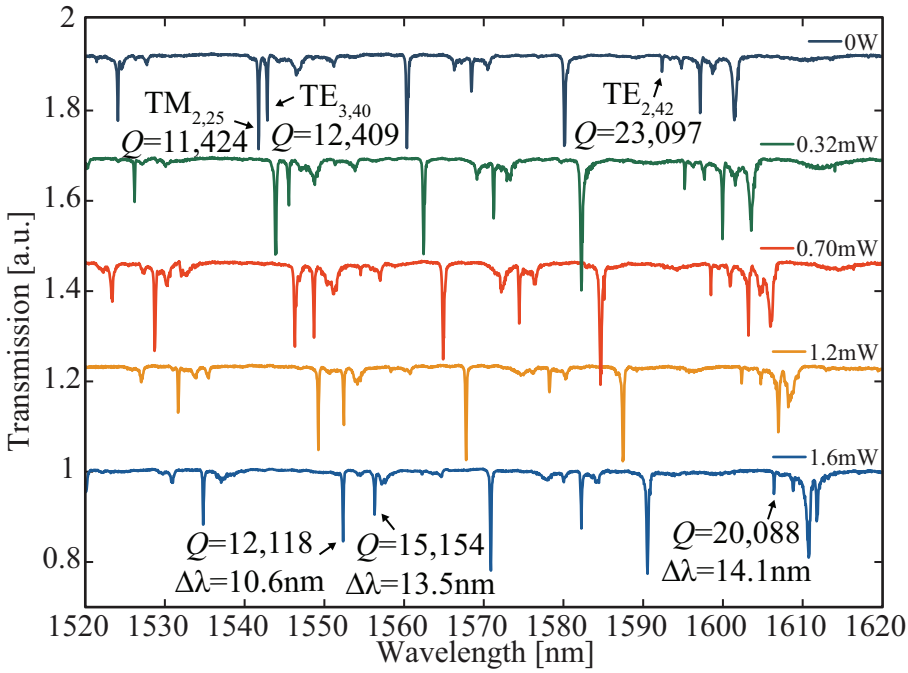

Fig. 2. (Color online) Tapered fiber spectra of a tunable microdisk. Spectra are shown at tuning powers from 0W to 1.6mW. Several prominent peaks are labeled and their behavior characterized.

deep-UV lithography.

3. Experimental characterization and analysis

The optical properties of the microdisks were characterized using tapered-fiber spectroscopy [7, 14, 16, 17]. With this technique, the evanescent field of the fiber optical mode couples to the microdisk, and resonances are identified as dips in the fiber transmission spectra. Q factors are obtained by fitting the experimental data to a Lorentzian.

Figure 2 shows tapered fiber spectra obtained from a 10μm tunable silicon microdisk. The first spectrum had zero applied voltage. The following scans had 10V, 15V, 20V, and 25V respectively. The resonances are seen to shift by 10nm-14nm. Several prominent features have been labeled and their characteristics analyzed in more detail. The $TM_{2,25}$ mode initially at 1541.77nm shifts to 1552.35nm with 1.6mW of joule heating, a shift of 10.58nm. The Q factor of this mode is measured to be 11,424 in the first spectrum and 12,118 in the final spectrum. These measured Q factors depend significantly on loading from the fiber [14, 17], and the discrepancy between these two numbers is likely due to minor shifts in the fiber position between the two measurements. The actual unloaded Q is surely higher than in these measurements. In contrast to this TM mode, the $TE_{3,40}$ mode initially at 1542.82nm shifts 13.51nm to 1556.33nm and has a Q factor of $\sim 15,000$ throughout the measurements. The mode observed to have the largest shift and highest Q was the $TE_{2,42}$ mode initially at 1592.38nm and moving to 1606.45nm, a shift of 14.07nm. The Q of this mode was around 20,000 in all measurements, and was measured to have the highest Q in the first spectrum at 23,097. In the final spectrum the measured Q was 20,088. The presence of a multitude of modes with Q factors exceeding

#127156 - $15.00 USD Received 20 Apr 2010; revised 28 May 2010; accepted 7 Jun 2010; published 21 Jun 2010

10,000 and some exceeding 20,000 is a strength of this structure and shows that the perturbation due to the electrodes does not degrade the cavity below a functional level.

It is important to understand the various contributions to the measured Q factors. The measured Q will have several contributions, as described by Eq. 1.

$$Q_{\mathrm{M}}^{-1} = Q_{\mathrm{D}}^{-1} + Q_{\mathrm{C}}^{-1} + Q_{\mathrm{P}}^{-1}. \tag{1}$$

Here Q_{M} is the measured Q factor obtained by fitting a Lorentzian function to the tapered fiber data. Q_{D} is the contribution to the Q factor resulting from mechanisms associated with the extra electrons in the material due to doping of the substrate. Q_{C} is the contribution due to scattering by the contacts. Q_{P} contains all other parasitic contributions such as scattering due to sidewall roughness not associated with the contacts as well as loading due to the tapered fiber waveguide. We have obtained estimates for each of these experimentally by studying different systems with isolated variables. To estimate Q_{P} we have studied microdisks made with the same fabrication techniques but on substrates without doping and with no contacts in the sidewalls for tuning. In our experiments the measured Q factors of these structures were 40,000-230,000 depending on the specific sample and mode. While it is quite possible to obtain substantially higher Q factors in silicon microdisks [16], doing so necessitates a different choice of electron beam resist and an additional resist reflow step. This reflow is incompatible with our fabrication of nanowire contacts. To estimate Q_{C} we again utilized the undoped SOI, but fabricated wired microdisks on the substrates. In these structures Q factors ranging from 15,000-47,000 were measured. Assuming $Q_{\mathrm{P}} = 230,000$ and $Q_{\mathrm{D}} = \infty$, this gives $Q_{\mathrm{C}} = 59,000$ for the mode of highest-Q measured in a wired microdisk without doping. To estimate Q_{D} we have measured the Q factors of disks created from the doped SOI substrates but without contacts for tuning. In these structures the measured Q factors were in the range of 17,000-50,000, but few exceeded 30,000. We can use these data to make educated guesses about the different contributions to the Q factors in the spectra shown in Fig. 2. For example, Assuming $Q_{\mathrm{P}} = 200,000$ and $Q_{\mathrm{D}} = 45,000$, using the value of $Q_{\mathrm{C}} = 22,000$ in Eq. 1 gives $Q_{\mathrm{M}} = 13,800$, roughly in agreement with the measured Q factor of the $\mathrm{TE}_{3,40}$ mode shown in Fig. 2. Using the same values for Q_{P} and Q_{D}, a value of $Q_{\mathrm{C}} = 47,000$ gives $Q_{\mathrm{M}} = 20,600$, which agrees well with the lowest measured value of the Q factor of the $\mathrm{TE}_{2,42}$ mode. It is important to note that while these numbers give estimates for the various contributions to the measured Q factors in these experiments, there is a great deal of room for improvement in future devices both in optimization of the dopant dosage, the contact geometry, and the fabrication, as discussed in Sec. 2.

We further analyze the data in Fig. 2 to gain insight into the relationship between mode shift and polarization. Figure 3(a) is experimental data of wavelength shift versus power for fifteen modes including modes of both polarizations and various radial orders. Figure 3(b) is a theoretical plot of wavelength shift versus power and index of refraction calculated numerically [14]. The temperature of the disk was determined as a function of power dissipated to joule heating using the Comsol simulation shown in Fig. 1(b). This temperature was then related to the index of refraction through the thermooptic coefficient. The Comsol simulations give values for the power which are nearly a factor of two greater than the measured values. This is likely due to minor discrepancies in the geometry and material parameters used in the simulations. In both the theoretical and experimental cases, the modes are seen to separate into two distinct groups depending on the polarization with TE modes shifting $\sim$25% more than TM modes. This dependence on polarization was not observed to depend on radial mode order and can be understood by consideration of the fraction of electrical energy stored in the cavity. This quantity is given by

$$\xi = \frac{\int_{\mathrm{disk}} \varepsilon(\mathbf{r})|\mathbf{E}(\mathbf{r})|^2 d\mathbf{r}}{\int_{\mathrm{all\ space}} \varepsilon(\mathbf{r})|\mathbf{E}(\mathbf{r})|^2 d\mathbf{r}}. \tag{2}$$

#127156 - $15.00 USD Received 20 Apr 2010; revised 28 May 2010; accepted 7 Jun 2010; published 21 Jun 2010

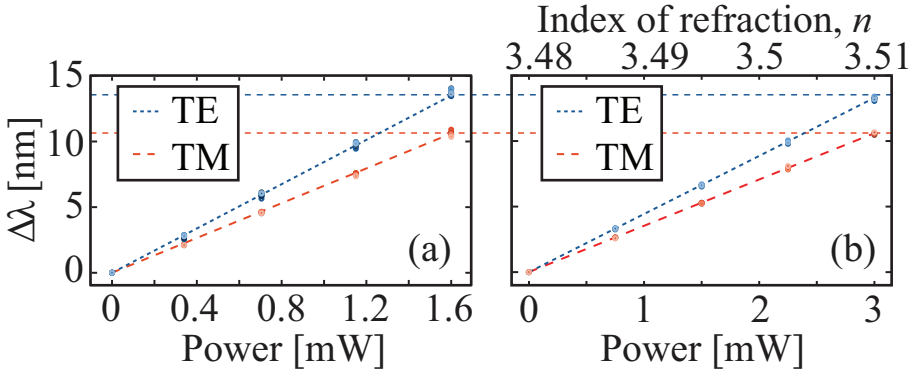

Fig. 3. (Color online) Difference in mode shifts between TE and TM polarized modes. (a) Experimental data of resonant wavelength shifts for fifteen modes of various radial orders as a function of power. TE and TM modes are seen to separate into distinct groups independent of radial mode order. (b) Theoretical prediction of mode shifts for six TE and six TM modes of various radial mode orders plotted as a function of power. The corresponding index of refraction labels the x-axis on the top.

We have calculated the quantity ξ given by Eq. 2 and the wavelength shift as n goes from 3.48 to 3.51 for six TE and six TM modes of various radial orders with wavelengths near 1550nm. For the TE modes the average value of ξ was 0.9796 with a standard deviation of 8.121×10^{-4}, and the average value of wavelength shift was 13.22nm with a standard deviation of 0.2798nm. For the TM modes the average value of ξ was 0.7836 with a standard deviation of 1.204×10^{-2}, and the average value of wavelength shift was 10.56nm with a standard deviation of 0.1701nm. The ratio of the average value of ξ to average value of wavelength shift is $7.409 \times 10^{-2}\text{nm}^{-1}$ for TE modes and $7.420 \times 10^{-2}\text{nm}^{-1}$ for TM modes. The similarity in these two values indicates that the predominant factor in dictating wavelength shift is the fraction of electrical energy stored within the cavity.

The difference in electrical confinement between modes of the two polarizations can be seen in Fig. 4 where we have plotted the magnitude of the electric field squared for characteristic second-radial order modes. Figure 4(a) shows the well-confined $\text{TE}_{2,42}$ mode, and Fig. 4(b) shows the $\text{TM}_{2,25}$ mode with prominent near field lobes forced outside the disk by the boundary conditions. The increased localization of TE modes within the disk relative to TM modes can be thought of as leading to an effective thermooptic coefficient which is the product of ξ with the bulk thermooptic coefficient of Si. For TE modes this is $1.82 \times 10^{-4}\text{K}^{-1}$ and for TM modes this is $1.46 \times 10^{-4}\text{K}^{-1}$. This difference in mode shift between the two polarizations has important consequences for applications which seek to utilize two nearby modes. By making use of this feature one can tune the spacing between two modes as well as the absolute position of each mode. It is also possible to tune two modes into or out of degeneracy.

4. Conclusions

In conclusion, we have presented a study of a tunable silicon microdisk structure. The tuning range was demonstrated to be as much as 14nm for TE modes and 10nm for TM modes. A Q factor exceeding 23,000 was observed for a mode that was tuned 14.07nm by the application of 1.6mW of power. The structures are made from standard SOI wafers in a single lithographic step. These tunable resonators have many potential applications in a wide range of on-chip photonic devices and have the potential to enable new systems with coupled electronic and

#127156 - $15.00 USD Received 20 Apr 2010; revised 28 May 2010; accepted 7 Jun 2010; published 21 Jun 2010

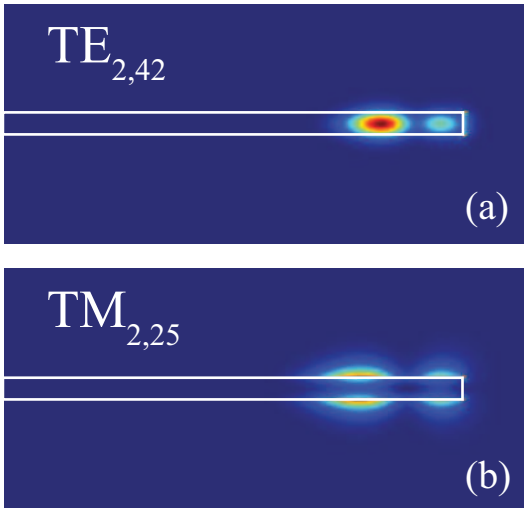

Fig. 4. (Color online) $|\mathbf{E}|^2$ calculated for the (a) $TE_{2,42}$ mode and (b) $TM_{2,25}$ mode. Field profiles are plotted in the $\rho - z$ plane and are assumed to have $\exp(im\phi)$ azimuthal dependence.

photonic degrees of freedom. Further, the fact that these tunable silicon resonators do not depend on the presence of a cladding layer for operation enables them to be used in a range of sensing applications.

Acknowledgments

We are grateful to Dr. Gernot Pomrenke and the grant support of AFOSR (FA9550-07-1-0286) and to the WCU program at SNU, Korea. This work was performed in part at the Center for Nanoscale Systems (CNS), a member of the National Nanotechnology Infrastructure Network (NNIN), which is supported by the National Science Foundation under NSF award no. ECS-0335765. CNS is part of the Faculty of Arts and Sciences at Harvard University.

#127156 - $15.00 USD Received 20 Apr 2010; revised 28 May 2010; accepted 7 Jun 2010; published 21 Jun 2010